Chapter 9

Ceramic Thick Films for MEMS

R.A. Dorey and R.W. Whatmore

Nanotechnology Group, School of Industrial and Manufacturing Science,
Cranfield University, Cranfield, Bedfordshire, UK, MK43 OAL

Many applications of ceramic thick films for MEMS have been highlighted in part A: applications and devices. While scaling of devices would appear to be a smooth transition, there are often fundamental changes in the nature of the fabrication processes used to realise devices with different thicknesses of ceramic film. Together with the chapters on thin films, this chapter aims to provide the reader with an understanding of some of the processes, and constraints, involved in processing of ceramic films for MEMS.

This chapter deals, specifically, with the fabrication of thick films where the film thickness is typically between 1 and 100 μm. The first part of this chapter provides an overview of the issues of interfacial reactions and constrained sintering which are typically associated with processing thick films. Interfacial reactions are often of concern due to the typical processing temperatures employed (600–1200 °C) and the associated high diffusion speeds of atomic species at these temperatures. The role of diffusion barriers in preventing interfacial reactions is discussed.

Following the overview of processing issues associated with thick films, a range of deposition techniques are reviewed. Screen printing, composite sol gel, electrophoretic deposition, thick film sol gel, direct writing, and ceramic paint are discussed.

The chapter concludes by offering a brief summary of typical thick films properties and thick film specific patterning techniques to compliment the chapters on material properties and processing.

1. Introduction

Micro-electromechanical systems (MEMS) containing active electroceramic components are of great importance in the fields of sensors, actuators and transducers [1, 2, 3]. There exist a number of active materials that exhibit useful piezoelectric responses. The most commonly used of these piezoelectric materials is lead zirconate titanate (PZT) [4] and many of the other systems also contain significant levels of lead. There are many issues that affect the processing of Pb rich materials such as the volatility and reactivity of Pb. It is the authors' intention to provide the reader with an overview of the different techniques for, and issues associated with, the production of functional oxide ceramic thick films/features. This article will also highlight some of the issues specifically associated with the production of Pb containing thick films due to the abundance of functional materials with high Pb contents.

Thick films are considered to be films ranging in thickness between 1 μm and 100 μm. They occupy a technological region between the processing capabilities of thin film deposition techniques and machining of bulk ceramics [1]. The ability to produce films in this range of thicknesses is of great importance due to the conflicting desires for greater miniaturisation, system integration and device power/sensitivity [5, 6].

Systems such as sensors, actuators and transducers require a certain thickness of active material in order to be sufficiently powerful/sensitive [7, 8] to be of commercial interest. Such thicknesses of material are not easy to fabricate using thin film production techniques such as sol-gel, sputtering, pulsed laser deposition (PLD), physical vapour deposition (PVD) or chemical vapour deposition (CVD) due to the slow deposition rates and high levels of stress generated during processing [9] which can lead to cracking of the film. Conversely the production, machining and bonding of bulk ceramics is not practical due to the expense, waste and difficulty in handling the ceramics [10]. Thick film fabrication routes allow the possibility of directly integrating the films onto the substrate so eliminating the difficulty of handling thin fragile ceramic components.

The two main issues associated with the processing of ceramic thick film materials are those of material compatibility (interfacial reactions) and constrained sintering. These are unique problems faced by thick film processing techniques due to the high processing temperatures and the presence of the substrate.

2. Common Issues with Thick Film Production

2.1. Interfacial reactions

2.1.1. Substrate materials

Thick film fabrication, like bulk ceramic processing, is based on powder processing routes and as such requires high processing temperatures in order to be able to densify the films. One of the issues associated with this need for high processing temperatures is the selection of an appropriate substrate material to support the film and form the MEMS. The easiest solution to this problem is to use a thermally and chemically stable substrate such as polycrystalline alumina or sapphire. However, these materials are
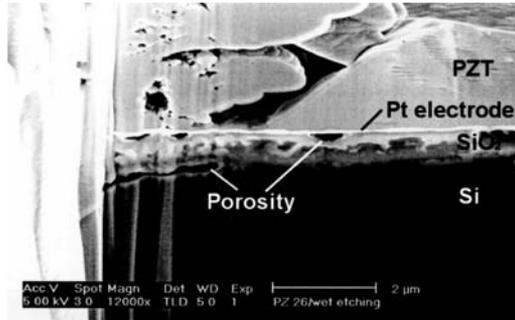
Fig. 1. Example of reaction between Si and Pb (within the SiO$_2$ layer) during the processing of a PZT thick film.

difficult to process (they are hard and chemically inert), can be expensive and there is little micromachining know-how relating to them. Instead there is a considerable drive to integrate the functional oxide ceramic thick films with silicon [11, 12], silica (glass) [13, 14] and metals [9, 15] such as steel, iron, chrome, nickel, copper and cobalt. These materials are of great interest as they are readily available, inexpensive, easy to machine and, in the case of metals, ductile [15]. The use of these materials in conjunction with thick film oxide ceramics is, however, limited by their upper processing temperature capabilities of approximately 900 °C [16, 17] and undesirable reactions between the substrate and film (i.e. lead and silicon) [18, 19].

2.1.2. Diffusion barriers

Diffusion barriers are often deposited onto the surfaces of substrates to prevent interdiffusion of atomic species between the substrate and film. Although silicon can be processed at temperatures as high as 900 °C it has been shown that deleterious reactions can occur between silicon and lead [7, 20, 21] at much lower temperatures (figure 1). During the sintering of Pb containing films on silicon, Pb was found to diffuse readily through SiO$_2$ or Si$_3$N$_4$ layers [22] on the surface of silicon, leading to the formation of lead silicate compounds at the silicon / PZT interface, delamination, and increases in the conductivity of the SiO$_2$ layer [22, 23]. Such diffusion of the lead species is often enhanced by the presence of a liquid phase [17, 21].

The use of diffusion barriers has been employed to separate the silicon and lead containing materials and to prevent the migration of atomic species. The requirements of a diffusion barrier are that it should resist the passage of atoms though it, it should not be a weak link through poor adhesion to the substrate or film, and it should be as thin as possible so as not to affect the performance of the device as a whole. Examples of successfully implemented thin diffusion barriers on silicon include 70 nm yttria stabilized zirconia (YSZ)/30 nm TiO$_2$ [24], 120 & 150 nm ZrO$_2$ [25, 19], 350 nm TiO$_2$[26], 300 nm MgO [19], Rh/TaN [27]. Thick film diffusion barriers have also been employed to yield satisfactory results. i.e. 1 μm columnar YSZ [28], 1 μm SiO$_2$/50 nm TiO$_2$/500 nm Pt [7].

2.1.3. Electrode materials

There are a limited number of suitable materials available for use as back electrodes. These electrodes are deposited onto the substrate prior to the deposition of the active electroceramic component and must therefore be able to withstand the processing temperatures used during the processing of the electroceramic and remain electrically conducting. Pt, Au, and Au/Pt/Pd [15], Ag/Pd [29] alloys have been shown to be effective back electrodes as they do not oxidise at the high processing temperatures. However, reactions between Si and Au, with the formation of a Si-Au eutectic [23], have been reported. This effectively limits the use of Au in conjunction with silicon substrates.

The alloy systems tend to be applied using a screen printing process and are themselves relatively thick (1–2 μm) which may limit their use in certain applications. The thickness of such an electrode does in itself act as an effective diffusion barrier. The use of Pt electrodes is limited to below 850 °C as the electrodes tend to degrade due to the large thermal expansion mismatch between silicon and Pt and the enhanced creep characteristics of Pt at elevated temperatures which result in the formation of islands and/or nodules [15, 30]. To enhance the adhesion between the substrate and the Pt electrode a thin (5–20 nm) Ti or TiO_2 adhesion layer is often used.

A reduction in processing temperature to below 800 °C could increase the range of materials that would be suitable for use as back electrodes. Possible alternative metals could include less noble metals such as Cr, Al, Cu [15]. An alternative approach to using noble metals as electrodes is to utilise a conducting ceramic such as RuO_2. [31].

2.2. Constrained sintering

2.2.1. Shrinkage

One of the key issues associated with the production of any coating on a rigid substrate is that of shrinkage. Constrained shrinkage occurs when the coating undergoes a reduction in volume while the dimensions of the substrate remain unchanged. This occurs initially during the drying of the film when fluid between the ceramic particles is removed through evaporation. A further volume reduction occurs during the sintering of the ceramic particles when pores are eliminated. In an unconstrained body the volume reduction is accomplished via isotropic shrinkage. However, when the film is supported on a rigid substrate the shrinkage in the plane of the film (x + y) is prevented [32]. This leads to the generation of in-plane tensile stresses within the film. The principles dictating constrained shrinkage during drying and sintering are comparable. The primary difference being that during the early stage of drying there is sufficient fluid present to allow a degree of particle reorientation to relieve stress. Once a critical volume of fluid has been removed no further particle reorientation is possible and the situation can be likened to that of a film being sintered at very low temperature.

The general sintering behaviour of a 'green' film supported on a rigid substrate and subjected to a constant heating rate has been modelled by Zhao and Dharani [33] using a viscoelastic finite element simulation. Material properties, Young's modulus, and Poisson's ratio were assumed to be functions of density while the viscosity was taken to be a function of grain size, density and temperature. Density and grain size data
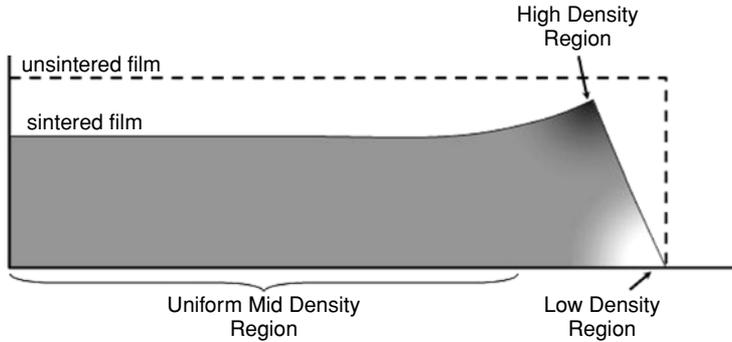
Fig. 2. Schematic of the general shrinkage behaviour of a constrained film during sintering.

were obtained from observations of unconstrained sintered samples. Zhao and Dharani modelled the effect of a range of films of different thicknesses fully constrained on a rigid substrate and found that the general sintered shape and density variations were consistent. A generalised schematic of these results is shown in figure 2.

The main body of a film was found to have a uniform density approximately midway between that of the unconstrained edge (highest density) and constrained edge (lowest density). For a 100 μm thick film the mean relative density of the constrained films was found to reach a maximum of 0.72 while that of unconstrained films was approximately 0.98. Although the form of the density variation was found to be comparable across the thickness ranges modelled, it was found that the maximum density attainable was lower for thinner films. The edge effect density variations predicted may prove to be an issue for MEMS processing where small features are required. This study was conducted assuming a constant heating rate and as such did not account for any effects of sintering time on the densification behaviour. Stech *et al.* [34] showed that for a TiO_2 film an appreciable degree of densification occurred during the first 150 minutes with higher densities attained at higher sintering temperatures. This observation indicates that relative densities greater that 0.72 could be attained if longer sintering times were employed. Although promising, care should be taken when applying these findings to the sintering of PZT thick films, as the use of longer sintering times and higher temperatures could lead to greater lead loss and a reduction in functional properties of the film. This is of particular concern as the surface area to volume ratio of films is higher that that of bulk ceramics and as such small levels of lead loss could have significant effects on the resultant functional properties. Kosec *et al.* [35] have demonstrated that the use of a Pb rich sintering atmosphere can be used to counter the evaporation of Pb during processing.

A finite element simulation of the effect of sintering time has shown that enhanced densification can be achieved if some form of stress relaxation can occur [36]. In a constrained film the generation of tensile in-plane stresses also give rise to shear stresses. Flow of material under the action of these shear stresses is able to bring about a reduction in the level of tensile stress (analogous to creep stress relaxation) as shown in figure 3. A non-dimensional relaxation parameter (ß—given by the ratio of the rate
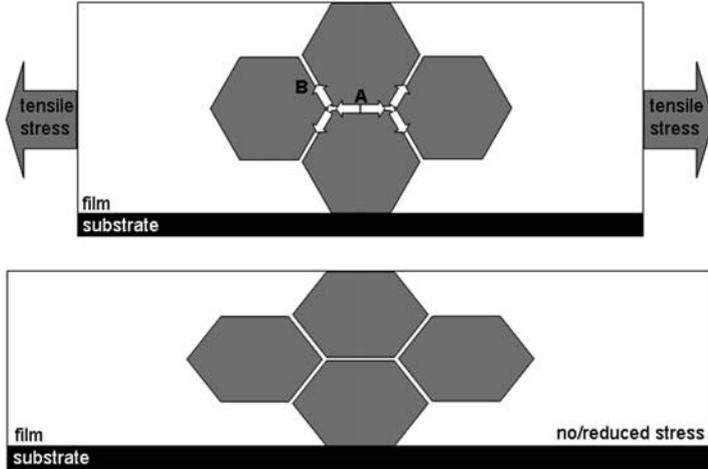
Fig. 3. Schematic of effect of a liquid phase sintering aid during sintering of thick films.

constant for shear diffusion and the rate constant for densification) was proposed to account for this stress relaxation.

The fundamental driving force for densification is given by the sintering pressure p:

$$p = -\frac{(\sigma_x + \sigma_y + \sigma_z)}{3} \tag{2.1}$$

In an unconstrained film $\sigma_x = \sigma_y = \sigma_z = -p_o$. When the film is constrained, σ_x and σ_y are acted upon by the opposing constraint stress σ such that

$$\sigma_x - \sigma = \sigma_y - \sigma = -p_o \tag{2.2}$$

And equation 2.1 becomes:

$$p = p_o - 2/3\sigma \tag{2.3}$$

As the non-dimensional relaxation parameter, ß, $\to 0$ (i.e. no shear relaxation), $\sigma \to 3/2$ p_o and $p \to 0$ (i.e. no sintering). Conversely, if ß $\gg 1$ then $p \to p_o$ and the substrate has no effect on sintering. In reality ß is likely to be between the two extremes.

This analysis does provide a good indication of how the sintering of constrained films can be enhanced by encouraging the shear stress relaxation. If the diffusion controlled shear deformation can be enhanced then ß will increase and the degree of sintering will be greater. If densification and stress relaxation are controlled by grain boundary and lattice diffusion respectively then increases in the grain size and sintering temperature can lead to an increase in ß. However, care should again be taken if applying this to the PZT as discussed earlier. The analysis does provide an indication as to one possible way in which the application of sintering aids is beneficial to the sintering thick films. The sintering aid acts as a fast diffusion path for atomic species and also encourages the dissolution of material from areas of low stress (A) and the subsequent deposition of material at areas of high stress (B) (figure 3). A further route for stress relaxation is that of particle slippage whereby individual powder particles are able to move relative to

one another. This action would be enhanced by the presence of a liquid phase sintering aid [35] which acts as a lubricant allowing particles to slide over each other more easily. In a real system, both techniques are likely to be active. Particle slippage is likely to dominate during the early stages of sintering while the particles are still free to move. During the latter stages of sintering (and in the absence of sufficient liquid phase), when particles are less free to move, stress relaxation can be accomplished through diffusion controlled shear relaxation.

Reduced sintering rates are not the only effect that can occur due to constrained shrinkage. If the tensile stress generated during sintering (or drying) exceeds the fracture strength of the material then the film will crack. This is of particular importance if the density of the film is low (i.e. during drying, early stages of sintering and at constrained free edges) as the strength of the film will be severely reduced [32, 37]. Studies of the liquid phase sintering behaviour of ZrO_2 (with Bi_2O_3 sintering aid) and the solid state sintering of alumina have shown that the ZrO_2 which was able to undergo a degree of stress relaxation due to the liquid phase sintering aid did not crack during sintering [38].

Closely related to the effect of constrained shrinkage is that of thermal expansion mismatch which can also cause the film to crack. Large differences in the thermal expansion coefficients of the substrate and film will lead to the generation of tensile stresses in the film. These stresses will either arise during heating prior to sintering ($\alpha_{substrate} > \alpha_{film}$) or during cooling after sintering ($\alpha_{substrate} < \alpha_{film}$) [33]. Tensile stresses within the unsintered film are of greater concern due to the lower strength of the film. Hence care must be taken when using substrates with high thermal expansion coefficients (i.e. metals). Silicon and PZT, near the morphotropic phase boundary, both have thermal expansion coefficients in the region of 2×10^{-6} K^{-1} at temperatures below 500 °C [39, 40, 41] which helps to minimise the thermal expansion mismatch. At temperatures above 500 °C, and with non MPB composition PZT, significant thermal strains may arise.

2.2.2. Sintering aids

In solid state sintering of ceramic particles (in the absence of sintering aid) diffusion is slow even at high temperatures. The processing temperatures required to sinter a ceramic powder can be dramatically reduced through the addition of a liquid phase sintering aid. The liquid phase sintering aid initially facilitates the reorientation of the ceramic particles (acting as a lubricant) to allow a better degree of packing and increasing the density of the film. The liquid phase sintering aid also acts as a fast diffusion path for atomic species and encourages dissolution/reprecipitation of the ceramic so encouraging the densification process to occur.

The sintering temperature of bulk PZT is between 1100–1300 °C. Due to the high surface area to volume ratio of films it is very important to control the loss of volatile compounds. For this reason excess lead oxide and lead rich atmospheres are often employed when processing lead containing films. PbO has a melting point of approximately 850 °C and as such has been used as a sintering aid [27, 29, 42, 43]. Other examples of sintering aids used to reduce the processing temperatures to between 700 and 850 °C include PbO-Cu_2O [21, 44, 45], $Pb_5Ge_3O_{11}$ [46, 47, 48], $LiBiO_2$-CuO [49],

PbO-PbF$_2$ [10, 50, 51], Bi$_2$O$_3$-B$_2$O$_3$-CdO [10, 11, 52], Borosilicate Glass [11, 20, 22, 43], Li/PbO [53] and PbO/TiO$_2$ [54, 55, 56].

Although sintering aids significantly reduce the sintering temperature and enhance densification the presence of significant levels of non/low-function material within the thick film can reduce the resultant functional properties. Furthermore, as sintering aids enhance the degree of solution-reprecipitation of the major phase (i.e. PZT) there is a large degree of atomic mixing. This may affect the electromechanical properties of the ceramic. i.e. if a soft doped PZT is the major phase, but the sintering aid contains a significant proportion of hard dopants then the sintered PZT material will behave as a hard doped material. Care should therefore be taken when selecting the appropriate sintering aid.

3. Thick Film Deposition Techniques

3.1. Screen printing

Screen printing is the most widely used thick film deposition technique. During the printing process an ink is forced though a fine mesh to deposit it onto the desired substrate. The film is then dried and sintered at elevated temperatures to yield a dense thick film. One of the advantages associated with this technique is the ability to directly pattern the film by selectively masking certain areas of the mesh. This direct patterning eliminates the need to pattern (typically by etching) the film at a later stage. Limitations in the maximum resolution are imposed by the size of the mesh used; hence this technique may not be suitable for producing very fine features.

The screen printing ink is composed of 4 types of constituent which are thoroughly mixed to yield a homogenous product [54]. The 4 constituents are:

Functional Phase—this is composed of the material to be deposited (i.e. PZT).

Binder phase—this is typically a liquid phase sintering aid and is added in relatively small amounts (5–15 vol% relative to the functional phase). In addition to acting as a sintering aid it also helps to bind the functional phase together and to the substrate.

Carrier phase—this acts as support for the solid powders during the printing process. It typically represents between 20 and 40 vol% of the ink and is composed of volatile components (solvents) and non-volatile components (polymers). The solvents are removed during the initial drying stage to leave the polymers to temporarily bind the film together. During the burn out stage the polymers are removed to leave only the functional and binder phases in place.

Modifiers—these are added in small quantities to modify the rheological properties of the ink. These additions are again removed during the drying and burnout stages.

The mesh is constructed of stainless steel wire, or nylon, and is stretched across a frame. The pattern is produced by coating the mesh with a photosensitive emulsion and selectively exposing it to UV light. The unwanted material can then be removed to yield the patterned mesh. The mesh is positioned above (but not in contact with) the substrate and the ink placed on the mesh in front of a squeegee. The rheological properties of the ink are such that it does not pass though the mesh at this stage. The

squeegee is then drawn across the mesh forcing it into contact with the substrate. The action of shear stresses on the ink reduce its viscosity allowing it to flow though the open sections of the mesh. Once the squeegee has passed the mesh springs back from the surface of the substrate leaving the ink in place. The ultimate resolution of the screen printing process is limited by the resolution of the mesh and the flow of the ink once printed.

Once the ink has been printed it is dried to remove the solvents. At this stage further layers can be deposited to increase the film thickness if required. Once the film has been dried the organic components (i.e. polymers & modifiers) can be removed by a thermal treatment between 350 and 600 °C. A final sintering treatment of between 850 and 950 °C is then performed to densify the film. The burnout and sintering treatments are usually performed at the same time.

3.2. Composite film technology

Although thick films can be deposited by screen printing the technique is still based on the sintering of micron size ceramic particles which limits the minimum temperature that can be used to achieve dense products. To overcome this limitation, ceramic powder processing can be combined with low temperature sol-gel processing to yield a hybrid technique capable to producing thick films at low temperatures [44, 57, 58, 59, 60]. The process entails producing a composite slurry consisting of a ceramic powder and an oxide ceramic producing sol. The composite slurry is then deposited using a spin coating process whereby the electroded substrate wafer is coated with the slurry and spun at high speed to yield a thick film. The film is pyrolysed to convert the sol to an oxide ceramic and remove the organic components of the slurry. Successive layers can be deposited to increase the film thickness. A final sintering treatment above 600 °C is used to sinter the film and develop the functionality (i.e. perovskite phase in PZT). The resultant properties of the film are typically lower than those of the corresponding bulk ceramic (see table 1) due to the presence of significant levels of porosity. The incorporation of low melting point sintering aids [21, 44, 47] and repeated sol infiltration and pyrolysis [21] have led to significant improvements in the functional properties of these films to the point where the relative permittivity of films sintered at 710 °C are comparable to that of the bulk ceramic. The use of repeated sol infiltrations and low melting point sintering aids have allowed high density films to be produced at low temperatures [21] as shown in figure 4.

This technique has also been applied to a number of other deposition techniques including screen printing [25], dip coating [61], spray coating [62, 63], and interfacial polymerisation [64]. A variation of the composite sol-gel route is to use conventional thick film processing followed by infiltration of the oxide ceramic producing sol to increase the green density of the film [65]. Subsequent sintering is then enhanced due to the presence of the highly sinterable sol-gel derived nanophase.

3.3. Electrophoretic deposition

Electrophoretic deposition (EPD) is a simple, fast and inexpensive deposition technique for obtaining thick ceramic films. One of the advantages of EPD over other

Table 1. Comparison of values of relative permittivity for thick films and bulk ceramics (valued for tan δ have also been included where reported in the literature)

Thick film processing route	Processing temperature	ε (& tan δ) @ 1kHz		Ref
		Film	Bulk	
Screen print	1000 °C	204 (0.019)	560 (0.085)	50
Screen print	1050 °C	840 (0.0089)	2010–2050 (0.004)	10
Screen print	950–1030 °C	600–750	2100	6
Screen print	750–950 °C	400–750 (0.05)	*1100**	65
Screen print	750–950 °C	620–1024 (0.05)	*1100**	65
Screen print	900 °C	1500 (0.06)	2650 (0.04)	17
Composite film (screen)	710 °C	600	1200	25
Composite film (spin)	710 °C	1100 (0.02)	1200 (0.003)	21
Composite film (dip)	630 °C	1300 (0.2)	3240 (0.021)	61
Composite film (dip)	550 °C	2500	3240	100
Composite film (interface)	950 °C	771 (0.052)	1200	64
Microstereo lithography	700–850 °C	200 (0.01)		85

-estimated bulk values
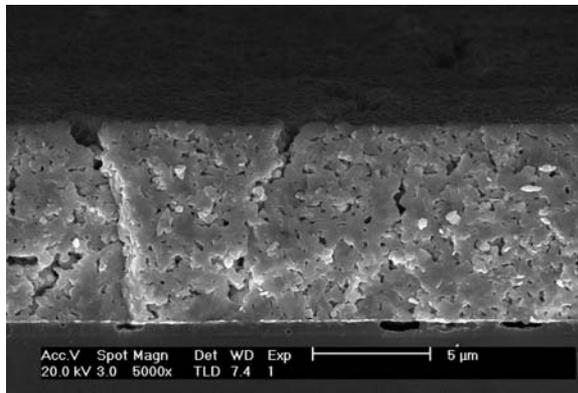
Fig. 4. Scanning electron microscope micrograph of a fracture cross-section of a high density composite film produced at 710 °C with sintering aid and repeated sol infiltration.

thick film deposition techniques is the ability to coat complex geometries [66]. The three stages to the process are the formation of a charged suspension, the deposition of charged particles onto an electrode under the action of a DC voltage and the final sintering [51, 53, 67].

The charged suspension can either be formed using electrosteric (dispersants) or electrostatic (pH control) stabilisation. In both cases a low concentration suspension is formed with a typical solids loading below 1 vol% [52]. The substrate is then set as a voltage relative to the reference electrode and the charged particles migrate under the action of the DC field. The field is either maintained at a constant value or adjusted so as to keep the current density constant [66]. Although conditions of constant current density are preferred, as this has the effect of maintaining a constant field in the suspension (and hence deposition rate), care must be taken not raise the voltage too high so as to avoid the evolution of gasses and/or heat at the electrodes which can lead to defects in the films [68].

Electrostatic suspension of PZT particles can readily be accomplished though the use of either acetic acid [53] or HNO_3/NH_3 [66]. Maintaining the pH of the suspension between 3 and 6 prevents the agglomeration of the PZT particles and associated reduction in deposition rate and production of poor quality films [66].

In order to deposit thick films using EPD it is necessary for the substrate to be conducting or coated with an electrode. This may act as a limitation for the use of this technique in the production of MEMS where often the ceramic film must also cover non-electroded (non-conducting) areas.

A further limitation is the high density of Pb containing compounds as it is very difficult to maintain large (i.e. heavy) particles in suspension. Tassle and Randall [53] found that PZT particles greater than 0.4 μm settled out of the suspension with those particles greater than 2 μm is size settling very rapidly. A consequence of this settling is the practice of operating EPD in a sideways or upwards deposition so that particles settling out of suspension do not contaminate the substrate.

A thorough review of the electrophoretic deposition technique, as applied to many ceramic oxide films, is given by Sarkar and Nicholson [69].

3.4. Thick film sol gel

While processing of oxide ceramic particle films does represent the main approach to realising thick films, conventional sol gel thin film chemistries have been modified to allow thick sol gel films to be fabricated. Thick sol gel processing makes use of alternative solvents such as diols [70, 71] which result in less rigid structures that are able to undergo stress relaxation with greater ease. Alternatively, additives which act both as strengtheners and plasticizers may be added to the system. Examples of such additives include polyvinyl pyrrolidine (PVP) [3, 72] and polyvinyl butral (PVB) [73]. These additives increase the strength by acting as 'long range' links holding the structure together during drying, and promote stress release by breaking up the polymeric gel network making the structure more flexible and able to deform plastically. With increased levels of additive the achievable thickness increases. However, increasing the levels of these additives also significantly increases the amount of organic material present. Hence, the structure may initially be capable of withstanding the shrinkage but it may fail when further shrinkage occurs when the additives are removed. These two conflicting effects on increasing the amount of plasticizer mean that there is an optimum level of addition where the greatest crack resistance is achieved. This optimum level of additions has been shown to be between 1 and 1.5 mol% [72] which yields a single

layer thickness of between 700 and 1500nm. This is much greater than that achievable using conventional sol gel techniques.

The ability to deposit such thick films brings with it its own issues. When the individual layers are this thick it is difficult to effectively remove the vapour/gases released as the film dries and the organic phase breaks down during pyrolysis. With standard thin film processing, the diffusion distances for gas to escape are relatively small. However, as the thickness increases so do the diffusion distances. This means that processing has to be conducted at a slower rate to allow time for the gas/vapour to escape. If the gas is unable to escape then pores will be formed which will decrease the properties of the film [74].

In thick sol gel films pores are generally formed at the bottom of the individual layers due to the greater diffusion distances required to effectively remove the gas and the constraining effects of the substrate (or layer below). When multiple layering is employed the resultant structure becomes one of alternating high and low density zones [75] with the pores trapped at the interface between individual layers. Despite the formation of these pores there is still considerable interest in developing sol gel materials that can be used to deposit films suitable for piezoelectric devices using a minimum number of layers.

A further complication associated with the processing of thicker films is that of compositional inhomogeneity arising from crystal growth. Ti rich PZT tends to nucleate in preference to Zr rich PZT [76, 77]. Hence, as the PZT crystal grows Zr is expelled from the perovskite lattice leading to an increase in concentration of Zr ahead of the crystal growth front. This Zr is gradually incorporated into the crystal lattice as the grain grows, leading to a variation in the ratio of Ti and Zr. Furthermore, local levels of lead may be reduced ahead of the growth front resulting in the formation of pyrochlore in place of perovskite PZT. This latter effect can be reduced by incorporating a slight (<10 at%) lead excess in the CSD film. The type of compositional variation differs depending on the manner in which the PZT nucleates and grows. If the PZT nucleates on the back electrode the resultant structure will be characterised by a rising Zr content as the distance from the back electrode increases. If intermediate crystallisation is carried out a 'saw toothed' distribution of Zr/Ti can be observed where a Ti rich material is observed at the base of each layer annealed [8, 76]. Depending on the level of Pb excess, an increase in Pb concentration may also be observed at the surface of the layers. This is caused by the expulsion of excess lead ahead of the crystal growth front [74, 76]. When the PZT nucleates at the back electrode and at the surface of the film, the middle of the layer is found to be Zr and Pb rich [74]. This is a result of the two growth fronts meeting in the centre of the film.

3.5. Direct writing

Recent developments in the field of direct writing have enabled a range of microscale devices to be created. Application of such technology has the benefit of eliminating the need to pattern the devices after deposition. Furthermore, the fact that the patterns are printed directly under computer control eliminates the need to make expensive photolithographic masks and screens, as well as increasing the flexibility of the system [78, 79]. Many of the direct writing technologies have been developed

through the continued refinement of existing macroscopic solid freeform fabrication techniques.

A number of micro-scale features have been produced using the ink jet printing technique. Ink jet printing is divided into two categories—continuous flow and drop on demand [80]. In the continuous flow process a steady stream of ink flows though a fine aperture. Rayleigh instability (assisted by the superimposition of a mechanical oscillation) causes the stream of ink to break up into single drops which can be deflected by a pair of charged plates. This technique has a faster deposition rate, but the need to deflect the ink drops elecrostatically requires that the ink be conductive [80, 81]. In drop on demand printing the ink drops are ejected from the print head when required (acoustic, mechanical or thermal ejection) and are positioned on the substrate by the mechanical movement of the print head relative to the substrate [80]. Both approaches require careful control of the ink to ensure good dispersion with no agglomerates or debris. Commercially available ink jet printers have a resolution of 1200 dpi ($\sim$20 µm).

The inks used for ink jet printing typically have a low solids loading (<5 vol%). The drying behaviour of the ink must be carefully controlled in order to maintain a high printing resolution. If the solvent evaporation is too slow the ink will spread on impact with the substrate leading to a loss of resolution. However if the ink dries too quickly then the printing nozzle may clog [82]. Typically a conventional ceramic ink drop with a diameter of 60 µm will spread to give a feature 600 µm wide and 1 µm high. Greater control of the feature size can be accomplished by reducing the volume of the ink drop [81] or by using an ink with a higher solids loading. Seerden *et al.* [80] have demonstrated that a ceramic ink with up to 40 vol% solids can be successfully printed using a drop on demand print head. By mixing the ceramic powder with a thermoplastic wax it was possible achieve alumina features with walls thinner than 100 µm. Other examples of features produced using drop on demand printing include 3 mm high ZrO_2 walls with widths of 340 µm [83] and ZrO_2 pillars 100 µm in diameter and 2 mm high [84].

Direct writing of patterns on substrates has also been accomplished using a micropen tool [78, 79] whereby a ceramic ink with 25–35 vol% solids loading is extruded through a pen. Related to the micropen is the technique of robocasting which again used a directable extrusion system to directly write a pattern on the substrate. The main difference between the systems is that robocasting using a more highly loaded ink (55–60 vol%) to produce lines approximately 575 µm wide. Both production techniques require a high temperature burn-out stage and a sintering stage to produce finished the product. Both robocasting and micropen rely on mechanically moving the delivery system or substrate and will therefore suffer the same mechanical control limitations imposed by the drop on demand ink jet printing technique.

Jiang et al. [85] have successfully produced PZT microfeatures on silicon substrates using a microstereolithographic process. Features between 10 and 150 µm thick and with line widths of between 20 and 100 µm were produced. This technique has also been used to fabricate small alumina gears 20 µm thick with diameters of approximately 400 µm and 1 mm [86]. To produce the PZT structures a PZT powder mixed with a UV curable monomer (1,6-hexabediol diacrylate (HDDA)), a photoinitiator (benzoin ethyle ether), solvent and dispersant to form a UV sensitive suspension with approximately 33 vol% solids loading. This suspension is then drawn across the substrate to leave a

uniform layer which is then selectively polymerised using a x-y scanning focused UV laser beam (Ar laser) with spot size of 1–2 μm. Control of the z position of the substrate allows further layers of suspension to be deposited and patterned. Once the required thickness has been obtained the unexposed areas were removed by washing with water and IPA. The PZT microfeatures were then subjected to a heat treatment designed to burn out the organic polymer (650 °C/4 hours) and sinter the PZT (700–850 °C/ 1–2 hours). The final electrical properties of the features were comparable to those of screen printed thick films. Structures with comparable feature sizes were produced using an alternative microstereolithographic process whereby a liquid crystal dynamic lithographic mask was placed in the path of the a columnated UV beam [87]. The resultant image is then reduced in size, using a lens, and focused onto the surface of the UV curable suspension. The thickness of the components is increased, as before, through successive deposition of further layers. The smallest feature size attainable was 50 μm with a resolution of approximately 5 μm.

A close relation of microstereolithography is gelcasting whereby a mould is first built up by selectively exposing a polymeric monomer to UV light as with microstere- olithography. Once the mould has been produced a suspension of ceramic particles in a polymer are cast into the mould and allowed to cure. The ceramic moulding is then heated to remove the organic components and to cause the ceramic to sinter. PZT microcomponents (with dimension ∼1cm in size) have been fabricated using this route [88]. The applicability of this technique for producing MEMS type components is ques- tionable due to the difficulty in ensuring thorough filling of the micro-scale moulds.

To date the use of direct write fabrication of MEMS systems has not become estab- lished due to the difficulties in operating at such small scales. Direct write fabrication techniques are readily capable of producing structures with feature sizes in the order of 100's of μm. For the direct fabrication techniques to be viable alternatives to the more established techniques it will be necessary to demonstrate the capability of producing feature sizes in the order of 10's of μm.

3.6. Paint

Related to the production of true ceramic thick films is the work being conducted on PZT thick film paints [89] which require no sintering process. Instead PZT is held in suspension in a liquid polymer which sets without the need for heat. The resultant properties of the thick films are significantly lower that those of conventional thick film materials, but there may be applications where piezoelectric thick films are required to be deposited at low temperatures.

4. Electrical Properties of PZT Thick Films

Due to the low processing temperatures and addition of significant levels of sintering aid the dielectric properties of PZT thick films are often significantly below those of the corresponding bulk ceramics. Table 1 gives details of the values of relative permittivity of thick films relative to those of the bulk ceramic (values of tan δ are also included where presented in the literature). Due to the large dependence of relative permittivity

on composition—in particular dopant additions—it is not practical to draw comparisons between the properties of different materials. Instead only those papers that reported the thick film relative permittivity along with those of the bulk ceramic are reported. Values of the $d_{33,f}$ piezoelectric coefficient which were reported were between 1/4 and 1/3 those of the bulk ceramic [6, 10, 65, 85]. It should be noted that the value of $d_{33,f}$ is not only affected by the processing conditions, level of porosity and presence of sintering aid but also by the rigid substrate. The effect of the substrate clamping is to reduce the piezoelectric coefficient [90, 91] and to reduce the degree to which the film can be poled [91]. It is not the author's intention to go into greater detail. Instead the readers are directed to the appropriate references.

Although easy to measure and useful for determining the piezoelectric properties of the thick films, the d_{33} coefficient can give a misrepresentative idea of the piezoelectric capabilities of the thick film. Often thick films are used in bending mode devices where the d_{31} piezoelectric coefficient dictates the effectiveness of the material. Due to the small scale of the thick films it is not possible to measure the d_{31} piezoelectric coefficient directly using a standard Berlincourt type meter. A number of systems have been developed to measure the d_{31} piezoelectric coefficient by inducing a bending motion in a whole wafer [92]. The disadvantage of these systems is that the wafer must be fully coated and that only an average value of the piezoelectric coefficient can be obtained. An alternative approach [93] uses a modified Berlincourt meter, requires much smaller samples and can obtain localised values of d_{31}. Values of $e_{31,f}$ (strain equivalent of $d_{31,f}$) reported for a high density composite sol-gel film were between -4.5 and $-8 \, C/m^2$ [21] where calculated value of $e_{31,f}$ for the bulk ceramic was approximately $-16 \, C/m^2$. These values compare with those from a screen printed material which were typically less than $-1 \, C/m^2$ [25]. The enhanced properties were attributed to the high density and low level of non-functional material in the composite sol-gel films.

5. Patterning Thick Films

5.1. Material removal

The production of a uniform thick film, although of central importance for the manufacture of MEMS, does not represent the complete processing issues. As with the production of MEMS devices from thin film materials, the use of thick film materials also requires the shaping (patterning) of films. The primary differences between the patterning of thin and thick films arise due to two factors. The first, most obvious, is the increased volume of material that must be removed during patterning. The second difference is due to the different microstructures usually associated with the thick films.

Thin films are primarily etched using a form of reactive ion etching [94] allowing high side wall angles to be obtained due to the anisotropic nature of the etching. The disadvantage of these reactive ion etching techniques is the slow speed and need for dedicated machines when etching PZT (to prevent cross-contamination) [94]. This slow etch rate effectively prohibits the use of many of these thin film etching techniques for etching thick films on the grounds of the extremely long processing times required and the associated expense [94].
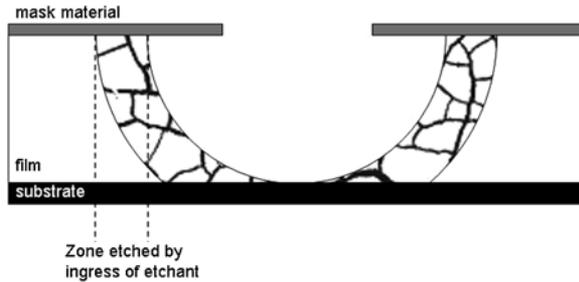
Fig. 5. Schematic representation of how porosity can lead to accelerated undercutting during wet etching.
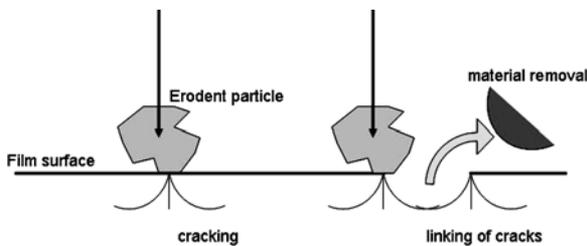

Fig. 6. Action of high speed particle on brittle substrate.

Thin films can also be etched using a wet chemical process. There are a number of etch recipes for etching PZT [94]. They are typically based around a HCl/HF mix where the HCl attacks the Ti and Pb components while the HF attacks the Ti and Zr components of the PZT. A number of further additions can also be added to the etchant to remove the insoluble Pb reaction products.

The high density of thin films, when made by sol-gel, PLD, sputtering, etc, lends itself to good edge control during wet etching. Due to the isotropic nature of wet etching it is only possible to obtain a 1:1 ratio between undercut and thickness [94]. The degree of undercutting for wet etching of thick films is generally greater due to the different microstructures of the thick films. These films, made using a route involving the consolidation of ceramic particles through the action of heat, usually have a higher degree of residual porosity. During etching, etchant can enter this porosity and accelerate the rate of undercutting (figure 5).

An alternative patterning technique that has successfully been employed for the production of thick film MEMS devices is that of powder blasting [28, 95]. Fine ceramic particles (3–30 μm) are accelerated under the action of high pressure gas and directed at the surface of the thick films. The particles impact the surface of the films at speeds of up to 290 m/s. When the high speed ceramic particles impact the surface of films the area directly under the particle is cracked (figure 6).

Repeated impacts lead to a network of cracks which link together allowing material removal to occur. The process is fast with relatively inexpensive equipment costs. Detailed patterns with features as small as 30 μm can be produced using this technique
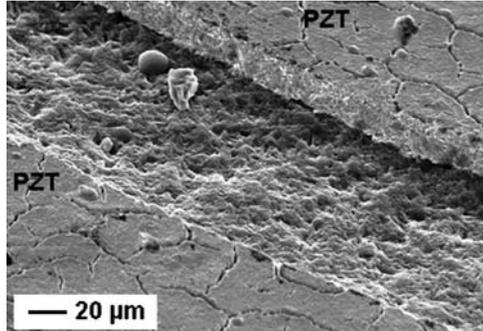
Fig. 7. SEM micrograph of an 80 μm wide trench powder blasted through a PZT thick film into a Si substrate [97].
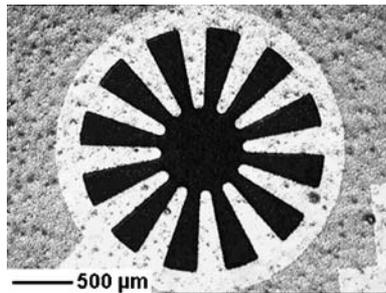

Fig. 8. A 1mm spoke test actuator formed by powder blasting into a PZT-on-silicon composite layer [28].

by selectively masking the surface of the films with a metal or elastomer mask [28, 96]. Powder blasting is particularly effective at eroding hard brittle materials and is well suited for patterning ceramics. However, there is limited selectivity between such hard materials. Due to the anisotropic nature of the process high aspect ratio holes can be produced. It is not possible to get perfectly straight side walls due to the interaction of the erosion particles with the edges of the mask. Figures 7 and 8 show features in a 10 μm thick composite sol-gel film obtained through powder blasting.

5.2. Direct patterning

The approaches adopted to yield a sol gel film that can be patterned are akin to those used with photoresist polymers. Sol gel chemistries have been modified so that the solubility of the system decreases [98, 99] when exposed to UV light. A decrease in solubility can be achieved through the use of beta-diketones with UV sensitive chelating rings which break on exposure to UV light [98] or through the use of photosensitisers or photoinitiators which cause enhanced crosslinking of the gel phase to occur on exposure to UV light [3, 99]. Such techniques have been used to produce patterned features with thicknesses in excess of 1 μm using a single deposition stage.

6. Conclusions

A number of established and emerging thick film deposition techniques have been presented. Although providing many ways to deposit thick films onto substrates the processes are all limited by the common reliance on oxide ceramic processing technology. The very nature of oxide ceramic processing necessitates the use of high processing temperatures to achieve effective densification. Very high processing temperatures can be avoided through the use of liquid phase sintering aid, small ceramic particles and repeated sol infiltration with the consequence that thick film processing can routinely be conducted in the range of 600–900 °C. This reduction in processing temperature is likely to increase the range of materials that can be successfully integrated into MEMS. It has already been demonstrated that the low temperature processing routes can be successfully used to deposit oxide ceramics onto low temperature substrates such as silicon and steel.

There exist two effective ways to pattern the thick film materials—wet etching and powder blasting. However, to obtain very high aspect ratio features for MEMS structures it will be necessary to further develop the direct patterning techniques for the deposition of these thick films. The current direct patterning technologies such as screen printing, stereolithography, ink jet printing are capable of producing features with dimensions in the order of 100 μm. This size range is at the upper border of MEMS processing and future developments within this field will increase the usefulness of these techniques within the filed of MEMS. The ability to realise feature sizes in the order of 10's of microns with comparable resolution will be the goal of future developments of direct write fabrication technologies.

There are still a number of challenges to be faced in the producing of thick film structures, but the continued refinement of current techniques, adaptation of unrelated technologies and development of wholly new approaches will be able to deliver the requirements needed for commercial thick film MEMS production.

7. Acknowledgements

References

[1] R.W. Whatmore, *Ferroelectrics*, **225**, 179, (1998)

[2] N. Setter, *J. Euro. Ceram. Soc.*, **21**, 1279, (2001)

[3] R.W. Whatmore, Q. Zhang, Z. Huang, and R.A. Dorey, *Materials Science in Semiconductor Processing*, **5**, 65, (2003)

[4] M. Koch, A. Evans, and A. Bunnschweiler, Microfluidic, *Technology and Applications* (Research Studies Press Ltd., Baldock, Hertfordshire, England), p137

[5] Y. Jeon, Y.G. Seo, S.-J. Kim, and K. No, *Integrated Ferroelectrics*, **30**, 91, (2000)

[6] L. Simon, S. Le Dren, and P. Gonard, *J. Euro. Ceram. Soc.*, **21**, 1441, (2001)

[7] P. Glynne-Jones, S.P. Beeby, P. Dargie, T. Papakostas, and N.M. White, *Meas. Sci. Technol.*, **11**, 526, (2000)

[8] N. Ledermann, P. Muralt, J. Baborowski, S. Gentil, K. Mukati, M. Cantoni, A. Seifert, and N. Setter, *Sensors and Actuators A*, **105**, 162, (2003)

[9] Q.F. Zhou, H.L.W. Chen, and C.L. Choy, *Thin Solid Films*, **375**, 95, (2000)

[10] S. Le Dren, L. Simon, P. Gonnard, M. Troccaz, and A. Nicolas, *Mat. Res. Bull.*, **35**, 2037, (2000)

[11] E.S. Thiele, and N. Setter, *J. Am. Ceram. Soc.*, **83**, 1407, (2000)

[12] N. Setter, and R. Waser, *Acta mater.*, **48**, 151, (2000)

[13] E. Belloy, S. Thurre, E. Walckiers, A. Sayah, and M.A.M. Gijs, *Sensors and Actuators*, **84**, 330, (2000)

[14] D. Mülsenberg, *Microelectronics Journal*, **28**, 419, (1997)

[15] S.M. Spearing, *Acta mater.*, **48**, 179, (2000)

[16] E.S. Thiele, D. Damjanovic, and N. Setter, *J. Am. Ceram. Soc.*, **84**, 2863, (2001)

[17] M. Kosec, D. Murko, J. Holc, B. Malic, M. Ceh, T. Haike, and H. Beige, Z. Metallkd., **92**, 97, (2001)

[18] O.M. Kanunnikova, F.Z. Gilmutdinov, and A.A. Shankov, *International Journal of Hydrogen Storage*, **27**, 783, (2002)

[19] Y. Jeon, J. Chung, and K. No, *J. Electroceram.*, **4**, 195, (2000)

[20] S.P. Beeby, A. Blackburn, and N.M. White, *J. Micromech. Microeng.*, 9, pp. 218–229, (1999)

[21] R.A. Dorey, S.B. Stringfellow, and R.W. Whatmore, J. Euro. Ceram. Soc., **22**, 2921, (2002)

[22] R. Maas, M. Koch, N.R. Harris, N.M. White, and A.G.R. Evans, *Materials Letters*, **31**, 109, (1997)

[23] M. Koch, N. Harris, R. Maas, A.G.R. Evans, N.M. White, and A. Brunnschweiler, *Meas. Sci. Technol*, **8**, 49, (1997)

[24] Y.B. Kim, T.S. Kim, K.S. Choi, and D.J. Choi, *Integrated Ferroelectrics*, **35**, 199, (2001)

[25] R.A.Dorey, R.W. Whatmore, S.P. Beeby, R.N. Torah, and N.M. White, Integrated Ferroelectrics, Integrated Ferroelectrics, **54**, 651, (2003).

[26] F.F.C. Duval, R.A. Dorey, and R.W. Whatmore, *Thin Solid Films*, in press

[27] T. Futakuchi, K. Nakano, and M. Adachi, *Jpn. J. Appl. Phys.*, **39**, 5548, (2000)

[28] S. A. Wilson, R. D. Haigh, J. E. A. Southin, R. A. Dorey, and R. W. Whatmore, *Proceedings of Euspen 03*, Aachen, Germany, 19–20 May, (2003)

[29] V. Farrari, D. Marioli, A. Taroni, and E. Ranucci, *Sensors and Actuators B*, **68**, 81, (2000)

[30] P. D. Hren, S.H. Rou, H.N. Al-Shareef, M.S. Ameen, O. Auciello, and A.I. Kingon, *Integrated Ferroelectrics*, **2**, 311, (1992)

[31] B. Wang, K.W. Kwok, HJ.L.W. Chan, C.L. Choy, K.Y. Tong, E.Z. Luo, J.B. Xu, and I.H. Wilson, *Materials Characterisation*, in press

[32] S.-Y. Tzeng, and J.-H. Jean, *J. Am. Ceram. Soc.*, **85**, 335, (2002)

[33] Y. Zhau, and L.R. Dharani, *Thin Solid Films*, **245**, 109, (1994)

[34] M. Stech, and P. Reynders, and J. Rodel, *J. Am. Ceram. Soc.*, **83**, 1889, (2000)

[35] M. Kosec, J. Holc, B. Malic, and V. Bobnar, *J. Euro. Ceram. Soc.*, **19**, 949, (1999)

[36] R.K. Bordia, and R. Raj, *J. Am. Ceram. Soc.*, **68**, 287, (1985)

[37] R.K. Bordia, and A. Jagota, *J. Am. Ceram. Soc.*, **76**, 2475, (1993)

[38] T. J. Garino, and H.K. Bowen, *J. Am. Ceram. Soc.*, **70**, C315, (1987)

[39] T. Mitsui, M. Marutake, E. Sawaguch, *in Landolt-Börnstein Numerical data and functional relationships in science and technology, Volume 9, Suppliment and Extansion to volume 3, Ferro- and antiferroelectric substances*, ed. K.-H. Hellwege and A.M. Hellwege (Springer-Verlag, Berlin, 1975) p. 309

[40] D. Berlingcourt, H.H.A. Krueger, and C. Near, *Technical publication TP-226, Properties of Piezoelectricity Ceramics* (Morgan Electro Ceramics, www.morgan-electroceramics.com)

[41] Y. Okada, and Y. Tokumara, *J. App. Phys.*, **56**, 314, (1984)

[42] G. De Cicco, B. Morton, D. Dalmonego, and M. Prudenziati, *Sensors and Actuators*, **76**, 409, (1999)

[43] M. Prudenziati, B. Morten, and De Cicco, *Microelectronics international*, **38**, 5, (1995)

[44] D.L. Corker, Q. Zhang, R.W. Whatmore, and C. Perrin, *J. Euro. Ceram. Soc.*, **22**, 383, (2002)

[45] D.L. Corker, R.W. Whatmore, E. Ringgaard, and W.W. Wolney, *J. Euro. Ceram. Soc.*, **20**, 2039, (2000)

[46] P. Tran-Huu-Hue, F. Levassort, F.V. Meulen, J. Holc, M. Kosec, and M. Lethiecq, *J. Euro. Ceram. Soc.*, **21**, 1445, (2001)

[47] T. Hayashi, T. Inoue, and Y. Akiyama, *J. Euro. Ceram. Soc.*, **19**, 999, (1999)

[48] F.F.C. Duval, R.A. Dorey, Q. Zhang, and R.W. Whatmore, *J. Euro. Ceram. Soc.*, J. Euro. Ceram. Soc., 23, 1935, (2003).

[49] X.X. Wang, K. Murakami, O. Sugiyama, and S. Kaneko, *J. Euro. Ceram. Soc.*, **21**, 1367, (2001)

[50] C. Lucat, F. Menil, and R. Von Der Muhll, *Meas. Sci. Technol.*, **8**, 38, (1997)

[51] T. Sweeney, PhD Thesis, Cranfield University, UK, (1998)

[52] M.-C. Wang, M.-S. Huang, and N.-C. Wu, *J. Euro. Ceram. Soc.*, **21**, 695, (2001)

[53] J. Van Tassel, and C.A. Randall, *J. Euro. Ceram. Soc.*, **19**, 955, (1999)

[54] M. Prudenziati, *Thick Film Sensors* (Elsevier, NL, 1994, ISBN 0444897232), p113

[55] Y. Jeon, Y.G. Seo, S.-J. Kim, and K. No, *Integrated Ferroelectrics*, **30**, 91, (2000)

[56] K. Kakegawa, T. Kato & Y. Sasaki, *J. Euro. Ceram. Soc.*, **20**, 1599, (2000)

[57] B. Kindl, D.J. Carlsson, Y. Deslandes, and J.M.A. Hoddenbagh, Ceramics International, **17**, 347, (1991).

[58] D.A. Barrow, T.E. Petroff, R.P. Tandon, and M. Sayer, *J. Appl. Phys.*, **81**, 876, (1997)

[59] D.A. Barrow, T.E. Petroff, and M. Sayer, Surface and Coatings Technology, **76–77**, 113, (1995)

[60] M. Lukacs, M. Sayer, and S. Foster, *Integrated Ferroelectrics*, **24**, 95, (1999)

[61] A.L. Kholkin, V.K. Yarmarkin, A. Wu, P.M. Vilarinho, and J.L. Baptista, *Integrated Ferroelectrics*, **30**, 245, (2000)

[62] T. Olding, M. Sayer, and D. Barrow, *Thin Solid Films*, **398–399**, 581, (2001)

[63] M. Kobayashi, T.R. Golding, M. Sayer, and C.-K. Jen, *Ultrasonics*, **39**, 675, (2002)

[64] T. Tsurumi, S. Ozawa, G. Abe, N. Ohashi, S. Wada, and M. Yamane, *Jpn. J. Appl. Phys.*, **39**, 5604, (2000)

[65] H.J. Kim, Y.-B. Kim, J.-Y. Kang, and T.S. Kim, *Integrated Ferroelectrics*, **50**, 11, (2002)

[66] J. Ma, and W. Cheng, *J. Am. Ceram. Soc.*, **85**, 1735, (2002)

[67] T.G. Sweeney, and R.W. Whatmore, *Ferroelectrics*, **187**, 57, (1996)

[68] B. Su, C.B. Ponton, and T.W. Button, *J. Euro. Ceram. Soc.*, **21**, 1539, (2001)

[69] P. Sarkar, and P.S. Nicholson, *J. Am. Ceram. Soc.*, **79**, 1987, (1996)

[70] N.J. Philips, S.J. Milne, *J. Mater. Chem.*, **1**, 893, (1991).

[71] R.W. Schwartz, T.L. reighert, P.G. Clem, D. Dimos, D. Liu, *Integrated Ferroelectrics*, **18**, 275, (1997).

[72] H. Kozuka, S. Takenaka, *J. Am. Ceram. Soc.*, **85**, 2696, (2002).

[73] Y. Takahashi, *Thin Solid Films*, **370**, 5, (2000).

[74] S. Sporn, S. Merklein, W. Grond, S. Seifert, S. Whal, A. Berger, *Microelectronic Engineering*, **29**, 161, (1995).

[75] K. Miyazawa, K. Ito, J. Mayer, M. Ruhle, *J. Am. Ceram. Soc.*, **81**, 2333, (1998).

[76] S.A. Impey, Z. Huang, A. Patel, R. Beanland, N.M. Shorrocks, R. Watton, R.W. Whatmore, *Journal of Applied Physics*, **83**, 2202, (1998).

[77] H.J. Willems, D.J. Wouters & H.E. Maes, *Microelectronic Engineering*, **29**, 217, (1995).

[78] B.H. King, D. Dimos, P. Yang, S.L. Morissette, *J.Electroceramics*, **3**, 173, (1999)

[79] S.L. Morissette, J.A. Lewis, P.G. Clem, J. Cesarano III, and D.B. Dimos, *J. Am. Ceram. Soc.*, **84**, 2462, (2001)

[80] K.A.M. Seerden, N. Reis, J.R.G. Evans, P.S. Grant, J.W. Halloran, and B. Derby, *J. Am. Ceram. Soc.*, **84**, 2514, (2001)

[81] P.F. Blazdell, and J.R.G. Evans, *J. Mater. Proc. Tech.*, **99**, 94, (2000)

[82] J.A. Lewis, *Current Opinion in Solid State and Materials Science*, **6**, 245, (2002)

[83] X. Zhao, J.R.G. Evans, and M.J. Edirisinghe, *J. Am. Ceram. Soc.*, **85**, 2113, (2002)

[84] X. Zhao, J.R.G. Evans, M.J. Edirisinghe, and J.H. Song, *J. Mater. Sci.*, **37**, 1987, (2002)

[85] X.N. Jiang, C. Sun, Z. Zhang, B. Xu, and Y.H. Ye, Sensors and Actuators, **87**, 72, (2000)

[86] X. Zhang, X.N. Jiang, and C. Sun, *Sensors and Actuators*, **77**, 149, (1999)

[87] M. Farsari, F. Claret-Tournier, S. Huang, C.R. Chatwin, D.M. Budgett, P.M. Birch, R.C.D. Young, and J.D. Richardson, *J. Mater. Proc. Tech.*, **107**, 167, (2000)

[88] D. Guo, K. Cai, C. Nan, L. Li, and Z. Gui, *Scripta mater.*, **47**, 383, (2002)

[89] J.M. Hale, and B. de Poumeyrol, *Proc. Ferroelectrics UK 2000*, 205, (2000), ISBN 1-86125-135-1

[90] M.-A. Dubois, and P. Muralt, *Sensors and Actuators*, **77**, 106, (1999)

[91] R.A. Dorey, and R.W. Whatmore, *Integrated Ferroelectrics*, **50**, 111, (2002)

[92] J.F. Shepard Jr, P.J. Moses, S. Trolier-McKinstry, *Sensors and Actuators A*, **71**, 133, (1998)

[93] J.E.A. Southin, S.A. Wilson, S. Schmitt, and R.W. Whatmore, *J. Phys. D:Appl. Phys.*, **34**, 1446, (2001)

[94] R.A. Miller, and J.J. Bernstein, *Integrated Ferroelectrics*, **29**, 225, (2000)

[95] H. Wensink, and M.C. Elenspoek, *Sensors and Actuators A*, **102**, 157, (2002)

[96] H. Wensink, H.V. Jansen, J.W. Berenschot, and M.C. Elwenspoek, **10**, 175, (2000)

[97] R.D. Haigh (2003), Private Communication

[98] N. Tohge and Y. Takama, *J. Mater. Sci.*, **10**, 273, (1999).

[99] S. Marson, R.A. Dorey, Q. Zhang, and R.W. Whatmore, *J. Euro. Ceram. Soc.*, **24**, 1925, (2004).

[100] A.L. Kholkin, V.K. Yarmarkin, A. Wu, M. Avdeev, P.M. Vilarinho, and J.L. Baptista, *J. Euro. Ceram. Soc.*, **21**, 1535, (2001)